WALAILAK JOURNAL
http://wjst.wu.ac.th Mathematics

Oscillatory Flow in a Vertical Channel Filled with Porous Medium with Radiation and Dissipation

Paresh VYAS[1] and Nupur SRIVASTAVA[2,*]

[1]*Department of Mathematics, University of Rajasthan, Jaipur 302004, India*
[2]*Department of Mathematics, Swami Keshvanand Institute of Technology, Management & Gramothan, Jaipur 302025, India*

([*]Corresponding author's e-mail: nupur2209@gmail.com)

Received: 18 June 2012, Revised: 10 December 2012, Accepted: 13 July 2013

Abstract

The present discussion is an analytical study of the oscillatory flow of a viscous incompressible Newtonian fluid in an infinite vertical parallel plate channel filled with porous medium. It is assumed that the flow is fully developed and the fluid is dissipative, gray, absorbing-emitting radiation and non-scattering. The radiative heat flux in the energy equation follows Rosseland approximation. It is considered that both the plates are stationary and temperature of one of the plates oscillates about a non-zero mean temperature. Approximate solutions to the coupled non-linear partial differential equations governing the flow have been found using the double perturbation technique. The effects of various parameters on the transient velocity, the transient temperature, the amplitude and phase of the skin friction and the rate of heat transfer have been analysed and shown in the form of graphs and tables.

Keywords: Unsteady, radiation, dissipation, vertical channel, porous medium, oscillatory temperature

Introduction

Every aspect of modern human life is inadvertently influenced by electronic equipments. The safety and reliability of such equipments is thus an important area of concern. Thermal control plays a very significant role in the proper design and control of the equipments which get excessively heated during their mode of execution. Electronic systems, especially low power systems, are conveniently cooled by free convection and radiation. In natural or free convection, fluid motion is caused by the density differences in a fluid produced due to temperature differences. The free convection velocities and free convection heat transfer rates are much smaller; hence this mode of convection has many thermal manufacturing applications, such as establishing temperature distributions within buildings, determining heat losses and heat loads for air conditioning systems. Geothermal reservoirs currently developed for commercial electric power generation are also characterized by the existence of natural convection within the systems. Comprehensive literature on various aspects of free convection flows and associated applications can be found in Ghoshdastidar [1], Nield and Bejan [2] and Incropera *et al*. [3].

Natural convection in vertical channels has been extensively studied because of its wide variety of engineering applications such as heat exchangers in solar domestic hot water systems, electronic cooling, design of passive solar systems for energy conversion, etc. Ostrach [4] was the first to report laminar natural convection flow in vertical channels with constant wall temperatures. Aung [5] studied the case when the plates were heated asymmetrically. Ample literature is found on heat and mass transfer effects in natural convection vertical channels with asymmetric boundary conditions (Miyatake *et al*. [6], Nakamura *et al*. [7], Aung *et al*. [8], Nelson *et al*. [9]). The influences of variable properties on flow and heat transfer behaviors have also been studied by many researchers (Hernandez *et al*. [10], Pantokratoras [11], Delmastro *et al*. [12]).

The modeling of convective flow through porous media is important from a practical viewpoint since it is required to predict the behavior of many systems. The process of natural convection in a porous medium is the driving mechanism in many geophysical situations where heat is convected to the earth's surface from an energy source deep below the ground. Free convection flows in porous geometries have been studied by Rudriah *et al*. [13] and Raptis *et al*. [14]. In recent years, porous media have been utilized in many high temperature applications, like the enhancement of heat transfer in coolant passages and many astrophysical systems. Radiative free convective flows in a porous medium have been analysed by Hossain *et al*. [15] and Raptis [16]. Oscillatory flows of viscous fluids over and through a porous medium has a wide variety of applications in the field of agricultural sciences, chemical engineering and petroleum technology. Free convective oscillatory flow through a porous medium has been discussed by Nanda *et al*. [17], Raptis *et al*. [18] and Makinde *et al*. [19]. Oscillatory two fluid flow in a horizontal channel in the presence of a magnetic field has been investigated by Umavati *et al*. [20].

In several practical applications, at high temperatures, heat losses by radiation from a surface are considerably high compared to that by natural convection. Radiative effects in porous medium over a stretching sheet have been studied by Vyas *et al*. [21,22]. Simultaneous heat exchange due to radiation and convection has equivalent importance, as it frequently occurs in many phenomena, like the flow of hot combustion products through cooled ducts, combustion, design of a furnace, in determining heat losses from a hot steam pipe passing from a room etc. Grief [23] analyzed laminar convective flow in a vertical heated channel. Radiation effects on free convection flows for an impulsively started vertical plate in a rotating fluid have been analyzed by Vijaylaksmi [24]. Unsteady natural convection has equal application in many technological processes and hence has been widely studied in different physical configurations (Kettleborough [25], Joshi [26], Paul *et al*. [27], Singh *et al*. [28,29], Andreozzi *et al*. [30]). Transient natural convection flow of a particulate suspension through a vertical channel has been studied by Mansour *et al*. [31].

Viscous dissipation plays an important role in various areas such as food processing, polymer manufacturing, geological processes in fluids contained in various bodies, and many others. The dissipative effects in porous media are due to shear stresses produced by the fluid itself, as well as due to the walls of porous matrix. Many studies have been reported in the literature about the expressions envisaging dissipation in porous media (see Nield [32] and Al-Hadhrami *et al*. [33]). Transient free convection flow between long vertical parallel plates, taking into account dissipation and oscillatory plate temperature, has been studied by Narahari [34].

Researching past literature identifies a need to investigate the conjunction of radiation, dissipation, free convection and oscillatory transient flow in a porous medium. The aim of the present paper is to consider the interactions of radiation and dissipation on the unsteady oscillatory fully developed flow in a vertical stationary channel filled with porous medium. Though dissipation is a quite weak effect compared to other counterpart effects, it certainly has a qualitative edge. A double perturbation technique is used to solve the coupled non-linear partial differential equations and obtain the analytical expressions for the transient velocity, transient temperature, skin friction coefficient and rate of heat transfer.

Materials and methods

A long parallel plate vertical channel consisting of stationary plates filled with a porous medium and having width h is considered. Cartesian system of coordinates is used, where x axis is taken along one of the plates and y axis is taken normal to it, as shown in **Figure 1**. The plate at y = 0 is at temperature $T = T_1$, while the temperature of the plate at y = h is given by $T = T_2 + \epsilon(T_2-T_1)e^{i\omega t}$, i.e. it oscillates about non-zero temperature T_2.

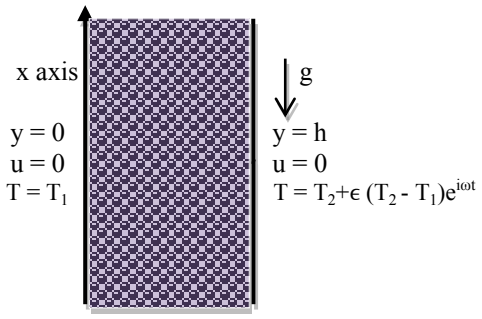

Figure 1 Schematic diagram of the problem.

Under Boussinesq's approximation, the unsteady flow of the viscous incompressible fluid within this channel is governed by the following system of partial differential equations;

$$\frac{\partial u}{\partial t} = g\beta(T - T_1) + \upsilon\frac{\partial^2 u}{\partial y^2} - \frac{\upsilon u}{k} \tag{1}$$

$$\rho C_p \frac{\partial T}{\partial t} = \kappa\frac{\partial^2 T}{\partial y^2} + \mu\left(\frac{\partial u}{\partial y}\right)^2 + \frac{\mu u^2}{k} - \frac{\partial q_r}{\partial y} \tag{2}$$

with the following boundary conditions;

$$\begin{aligned} &y = 0: \quad u = 0,\ T = T_1 \\ &y = h: \quad u = 0,\ T = T_2 + \varepsilon(T_2 - T_1)e^{i\omega t} \end{aligned} \tag{3}$$

where u is the fluid velocity, g is the acceleration due to gravity, β is the coefficient of volume expansion, T is the fluid temperature, υ is the kinematic viscosity, μ is the coefficient of viscosity, κ is the thermal conductivity, k is the permeability, ρ is the density, C_p is the specific heat at constant pressure and ω is the frequency of the oscillations of the plate temperature.

The radiative heat flux in the energy equation is given by;

$$q_r = -\frac{4\sigma_1}{3k_1}\frac{\partial T^4}{\partial y} \tag{4}$$

The temperature difference within the fluid is assumed to be sufficiently small so that T^4 may be expressed as a linear function of the temperature T. This is done by expanding T^4 in a Taylor series about T_1 and omitting higher order terms to yield.

$$T^4 \cong 4T_1^3 T - 3T_1^4 \tag{5}$$

The following non-dimensional quantities are introduced;

$$y^* = \frac{y}{h},\quad t^* = \frac{t\upsilon}{h^2},\quad u^* = \frac{u\upsilon}{h^2 g\beta(T_2 - T_1)} = \frac{uh}{Gr\upsilon},\ \omega^* = \frac{\omega h^2}{\upsilon},\ k^* = \frac{k}{h^2} \text{ and } \quad \theta = \frac{T - T_1}{T_2 - T_1} \tag{6}$$

Thus the governing equations in the non-dimensional form after dropping the asterisks become;

$$\frac{\partial u}{\partial t}=\theta+\frac{\partial^2 u}{\partial y^2}-\frac{u}{k} \tag{7}$$

$$\Pr\frac{\partial\theta}{\partial t}=(1+\frac{4N}{3})\frac{\partial^2\theta}{\partial y^2}+\Pr E\left(\frac{\partial u}{\partial y}\right)^2+\Pr E\frac{u^2}{k} \tag{8}$$

and the corresponding boundary conditions are;

$$\begin{aligned} &y=0: u=0, \quad \theta=0\\ &y=1: u=0, \quad \theta=1+\varepsilon e^{i\omega t}\end{aligned} \tag{9}$$

where the Grashof number Gr, Prandtl number Pr, Eckeret number E and Radiation parameter N are given by;

$$Gr=\frac{g\beta(T_2-T_1)h^3}{\upsilon^2},\quad \Pr=\frac{\mu C_p}{\kappa},\quad E=\frac{h^4g^2\beta^2(T_2-T_1)}{C_p\upsilon^2}=\frac{\upsilon^2Gr^2}{h^2C_p(T_2-T_1)},\quad N=\frac{4\sigma_1T_1^3}{k_1\kappa} \tag{10}$$

As the temperature of one of the plates is oscillating, hence the transient fluid velocity and transient fluid temperature are assumed as shown below, where $\varepsilon \ll 1$ is a small quantity;

$$u=u_0(y)+\varepsilon e^{i\omega t}u_1(y) \tag{11}$$

$$\theta=\theta_0(y)+\varepsilon e^{i\omega t}\theta_1(y) \tag{12}$$

Here u_0 is the mean velocity and u_1 is the fluctuating part of the velocity and θ_0 is the mean temperature and θ_1 is the fluctuating part of the temperature. We now substitute Eq. (11) and (12) in Eqs. (7) - (9), and neglect the coefficients of ε^2 and its higher powers, the harmonic and non-harmonic terms are equated to get;

$$u_0''=-\theta_0+\frac{u_0}{k} \tag{13}$$

$$u_1''-(i\omega+\frac{1}{k})u_1=-\theta_1 \tag{14}$$

$$\theta_0''=-\frac{\Pr E}{(1+\frac{4N}{3})}(u_0'+\frac{u_0^2}{k}) \tag{15}$$

$$\theta_1''-\frac{i\omega\Pr}{(1+\frac{4N}{3})}\theta_1=\frac{-2\Pr E}{(1+\frac{4N}{3})}(u_0'u_1'+\frac{u_0u_1}{k}) \tag{16}$$

with the boundary conditions;

$$\begin{aligned} &y = 0: \quad u_0 = 0, \quad u_1 = 0, \quad \theta_0 = 0, \quad \theta_1 = 0 \\ &y = 1: \quad u_0 = 0, \quad u_1 = 0, \quad \theta_0 = 1, \quad \theta_1 = 1 \end{aligned} \tag{17}$$

Eqs. (13) - (16) are coupled non-linear equations whose exact solutions are not possible. However, recalling that for incompressible fluids the Eckeret number $E \ll 1$, u_0, u_1, $\theta_0$and θ_1 are expanded in powers of E as;

$$\begin{aligned} &u_0 = u_{01} + Eu_{02} + O(E^2); \qquad u_1 = u_{11} + Eu_{12} + O(E^2) \\ &\theta_0 = \theta_{01} + E\theta_{02} + O(E^2); \qquad \theta_1 = \theta_{11} + E\theta_{12} + O(E^2) \end{aligned} \tag{18}$$

where $O(E^2)$ contains terms of E^2 and higher powers of E.
Substituting Eq. (18) into Eqs. (13) - (17) and equating coefficients of various powers of E, neglecting the terms of higher powers of E, the following system of equations is obtained.

$$u_{01}'' = -\theta_{01} + \frac{u_{01}}{k} \tag{19}$$

$$u_{02}'' = -\theta_{02} + \frac{u_{02}}{k} \tag{20}$$

$$u_{11}'' - (i\omega + \frac{1}{k})u_{11} = -\theta_{11} \tag{21}$$

$$u_{12}'' - (i\omega + \frac{1}{k})u_{12} = -\theta_{12} \tag{22}$$

$$\theta_{01}'' = 0 \tag{23}$$

$$\theta_{02}'' = -\frac{Pr}{(1 + \frac{4N}{3})}(u_{01}' + \frac{u_{01}^2}{k}) \tag{24}$$

$$\theta_{11}'' - \frac{i\omega Pr}{(1 + \frac{4N}{3})}\theta_{11} = 0 \tag{25}$$

$$\theta_{12}'' - \frac{i\omega Pr}{(1 + \frac{4N}{3})}\theta_{12} = \frac{-2Pr}{(1 + \frac{4N}{3})}(u_{01}'u_{11}' + \frac{u_{01}u_{11}}{k}) \tag{26}$$

Along with the corresponding boundary conditions;

$$\begin{aligned} &y = 0: \quad u_{01} = 0, \quad u_{02} = 0, \quad u_{11} = 0, \quad u_{12} = 0, \quad \theta_{01} = 0, \quad \theta_{02} = 0, \quad \theta_{11} = 0, \quad \theta_{12} = 0 \\ &y = 1: \quad u_{01} = 0, \quad u_{02} = 0, \quad u_{11} = 0, \quad u_{12} = 0, \quad \theta_{01} = 1, \quad \theta_{02} = 0, \quad \theta_{11} = 1, \quad \theta_{12} = 0 \end{aligned} \tag{27}$$

Solving Eqs. (19) - (26) and using boundary conditions (27);

$$\theta_{01} = y \tag{28}$$

$$u_{01} = ky - \frac{k\sinh(yk_1)}{\sinh(k_1)} \tag{29}$$

$$\theta_{02} = -\Pr N_1\left(\frac{k^2\cosh(2yk_1)}{4\sinh^2(k_1)} - \frac{2k^2 y\sinh(k_1 y)}{\sinh(k_1)} + \frac{2k^2\cosh(k_1 y)}{k_1\sinh(k_1)} + \frac{k^2y^2}{2} + \frac{ky^4}{12}\right) + T_1 y + T_2 \tag{30}$$

$$\begin{aligned} u_{02} = \Pr N_1\Big(&\frac{k^3\cosh(2k_1 y)}{12\sinh^2(k_1)} - \frac{k^2y^2\cosh(k_1 y)}{2k_1\sinh(k_1)} + \frac{3k^3 y\sinh(k_1 y)}{2\sinh(k_1)} - \frac{k^2y^4}{12} - \frac{3k^3y^2}{2} - 3k^4\Big) \\ &+ T_3\cosh(k_1 y) + T_4\sinh(k_1 y) + T_1 ky + T_2 k(1-y) \end{aligned} \tag{31}$$

$$\theta_{11} = \frac{\sinh(R_1 y)}{\sinh(R_1)} \tag{32}$$

$$u_{11} = \frac{1}{R_3}\left(\frac{\sinh(R_1 y)}{\sinh(R_1)} - \frac{\sinh(R_2 y)}{\sinh(R_2)}\right) \tag{33}$$

$$\begin{aligned} \theta_{12} = {} & T_5\cosh(R_1 y) + T_6\sinh(R_1 y) - \frac{2\Pr N_1}{R_3}\Big[\frac{ky\sinh(R_1 y)}{2\sinh(R_1)} - \frac{kR_2\cosh(R_2 y)}{R_3\sinh(R_2)} \\ & - \frac{kk_1R_1(\cosh(R_{10}y)/R_6 + \cosh(R_{12}y)/R_7)}{2\sinh(k_1)\sinh(R_1)} + \frac{kk_1R_2(\cosh(R_{11}y)/R_4 + \cosh(R_{13}y)/R_5)}{2\sinh(k_1)\sinh(R_2)} \\ & + \frac{y^2\cosh(R_1 y)}{4R_1\sinh(R_1)} - \frac{y\sinh(R_1 y)}{4R_1^2\sinh(R_1)} - \frac{y\sinh(R_2 y)}{R_3\sinh(R_2)} + \frac{2R_2\cosh(R_2 y)}{R_3^2\sinh(R_2)} \\ & - \frac{(\cosh(R_{10}y)/R_6 - \cosh(R_{12}y)/R_7)}{2\sinh(k_1)\sinh(R_1)} + \frac{(\cosh(R_{11}y)/R_4 - \cosh(R_{13}y)/R_5)}{2\sinh(k_1)\sinh(R_2)}\Big] \end{aligned} \tag{34}$$

$$u_{12} = \frac{2\,Pr\,N_1}{R_3}\Big[\frac{-ky\sinh(R_1y)}{2R_3\sinh(R_1)} - \frac{kR_1\cosh(R_1y)}{R_3^2\sinh(R_1)} - \frac{kk_1R_1}{2\sinh(k_1)\sinh(R_1)}\Big(\frac{\cosh(R_{10}y)}{R_{14}R_6} + \frac{\cosh(R_{12}y)}{R_{15}R_7}\Big)$$
$$+ \frac{kk_1R_2}{2\sinh(k_1)\sinh(R_2)}\Big(\frac{\cosh(R_{11}y)}{R_8R_4} + \frac{\cosh(R_{13}y)}{R_9R_5}\Big) - \frac{ky\sinh(R_2y)}{2R_3\sinh(R_2)} - \frac{y\sinh(R_1y)}{R_3^3\sinh(R_1)}$$
$$- \frac{\cosh(R_1y)(y^2 + 8R_1^2/R_3^2 + 2/R_3)}{4R_1R_3\sinh(R_1)} + \frac{(y\sinh(R_1y) + (2R_1/R_3)\cosh(R_1y))}{4R_1^2R_3\sinh(R_1)} - \frac{y(y\cosh(R_2y) - \sinh(R_2y)/R_2)}{4R_2R_3\sinh(R_2)} \qquad (35)$$
$$- \frac{1}{2\sinh(k_1)\sinh(R_1)}\Big(\frac{\cosh(R_{10}y)}{R_{14}R_6} - \frac{\cosh(R_{12}y)}{R_{15}R_7}\Big) + \frac{1}{2\sinh(k_1)\sinh(R_2)}\Big(\frac{\cosh(R_{11}y)}{R_8R_4} - \frac{\cosh(R_{13}y)}{R_9R_5}\Big) + \frac{y\sinh(R_2y)}{R_3^2\sinh(R_2)}\Big]$$
$$+ T_7\cosh(R_2y) + T_8\sinh(R_2y) + (T_5/R_3)\cosh(R_1y) + (T_6/R_3)\sinh(R_1y)$$

is obtained, where all the constants are listed in the Appendix. Now;

$$u_1(y) = M_r + iM_i$$
$$\theta_1(y) = T_r + iT_i \qquad (36)$$

are prescribed. The expressions for velocity and the temperature fields can be written in terms of real parts of the fluctuations of the unsteady velocity and temperature as;

$$u(y,t) = u_0(y) + \varepsilon(M_r\cos(\omega t) - M_i\sin(\omega t))$$
$$\theta(y,t) = \theta_0(y) + \varepsilon(T_r\cos(\omega t) - T_i\sin(\omega t)) \qquad (37)$$

Thus for $\omega t = \pi/2$, the expressions for the transient velocity and the transient temperature profiles are given by;

$$u(y,\pi/2\omega) = u_0(y) - \varepsilon M_i$$
$$\theta(y,\pi/2\omega) = \theta_0(y) - \varepsilon T_i \qquad (38)$$

The skin friction coefficient in a non-dimensional form at y = 1 is given by;

$$\tau = \left(\frac{du}{dy}\right)_{y=1} = \left(\frac{du_0}{dy} + \varepsilon e^{i\omega t}\frac{du_1}{dy}\right)_{y=1} = A + \varepsilon|B|\cos(\omega t + \alpha) \qquad (39)$$

where |B| is the amplitude of skin friction and α is the phase angle. Here;

$$B = B_r + iB_i \quad \text{and} \quad \tan\alpha = B_i/B_r \qquad (40)$$

The rate of heat transfer in non-dimensional form at the plate y = 1 is obtained as;

$$q = \frac{qh}{\kappa(T_2 - T_1)} = -\left(\frac{d\theta}{dy}\right)_{y=1} = -\left(\frac{d\theta_0}{dy} + \varepsilon e^{i\omega t}\frac{d\theta_1}{dy}\right)_{y=1} = C + \varepsilon|D|\cos(\omega t + \beta) \qquad (41)$$

where |D| is the amplitude of rate of heat transfer q and β is the phase angle. Here;

$$D = D_r + iD_i \quad \text{and} \quad \tan\beta = D_i / D_r \tag{42}$$

The constants appearing in τ and q appear in Appendix.

Results and discussion

Radiative dissipative transient free convection in a long vertical channel filled with incompressible fluid saturated porous material has been examined. A perturbation scheme has been developed to solve the coupled non-linear governing equations. The effects of various parameters on the transient velocity and transient temperature have been analyzed for two cases (air (Pr = 0.71) and water (Pr = 7)) and shown in the form of graphs (**Figures 2 - 12**).

Figures 2 and **3** show the variation in the transient velocity u with respect to the change in frequency ω for the case of air and water respectively. It is clear from these figures that for lower values of ω velocity increases with the increase in ω, while for higher values of ω the velocity decreases on increasing ω. **Figures 4** and **5** depict the velocity variation with respect to radiation parameter N for air and water, respectively. It is clear that as the radiation parameter N increases the velocity of air decreases, while that of water increases.

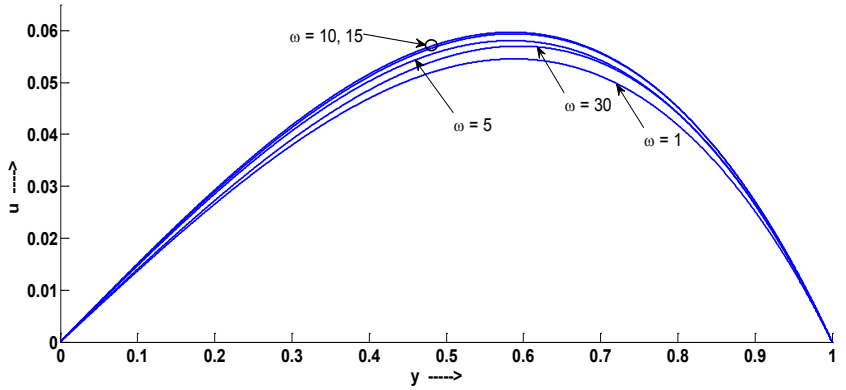

Figure 2 Velocity profiles for variation in ω when N = 2, E = 0.01, k = 0.5, ε = 0.2, Pr = 0.71.

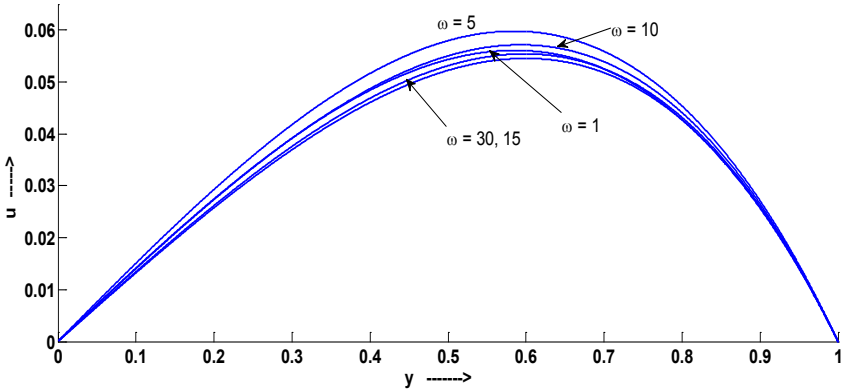

Figure 3 Velocity profiles for variation in ω when N = 2, E = 0.01, k = 0.5, ε = 0.2, Pr = 7.

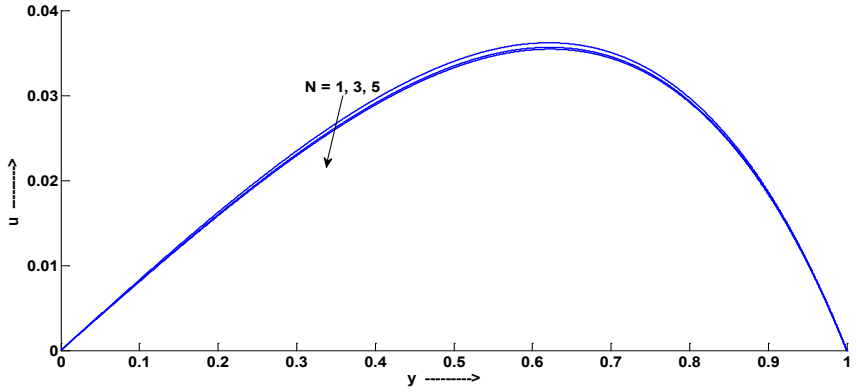

Figure 4 Velocity profiles for variation in N when ω = 10, E = 0.01, k = 0.1, ε = 0.2, Pr = 0.71.

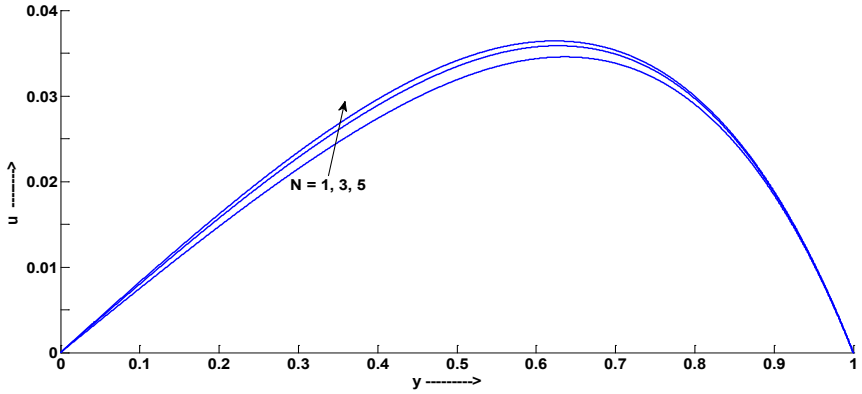

Figure 5 Velocity profiles for variation in N when ω = 10, E = 0.01, k = 0.1, ε = 0.2, Pr = 7.

The variation of velocity with respect to the permeability parameter k is shown in **Figure 6**. It clearly indicates that for both air and water, velocity of the fluid increases with the increase in permeability parameter k. The larger values of permeability indicate low resistance to fluid traversal inside the porous matrix. Hence, for larger values of permeability, a rise in velocity goes well with physics of the problem.

Figure 7 shows the variation of velocity with respect to the Prandtl number Pr and indicates that as the Prandtl number Pr increases, the fluid velocity decreases.

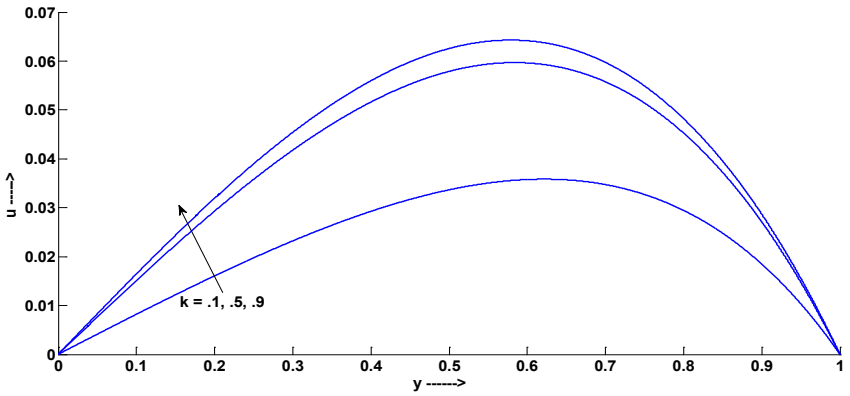

Figure 6 Velocity profiles for variation in k when ω = 10, E = 0.01, N = 2, ε = 0.2, Pr = 0.71/7.

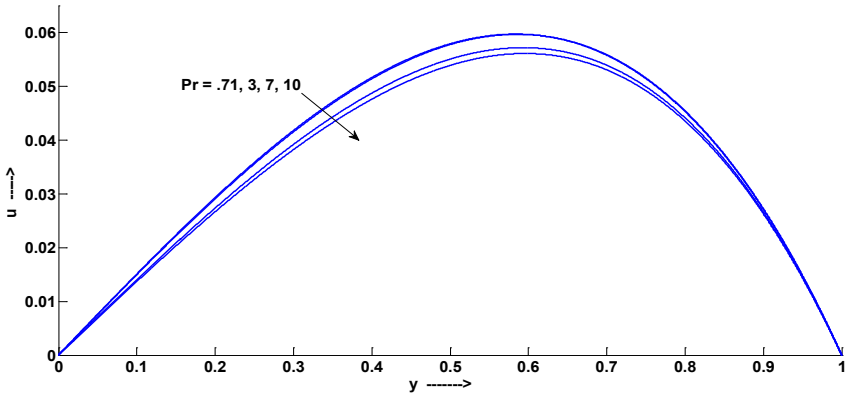

Figure 7 Velocity profiles for variation in Pr when ω = 10, E = 0.01, k = 0.1, ε = 0.2, N = 2.

Figures 8 and **9** show the variation of temperature θ with respect to frequency ω for the 2 cases of air and water, respectively. **Figure 8** shows that as ω increases the temperature of air increases; the temperature of water first increases and then decreases. Moreover, in the case of water temperature, fluctuations are important towards the oscillating plate.

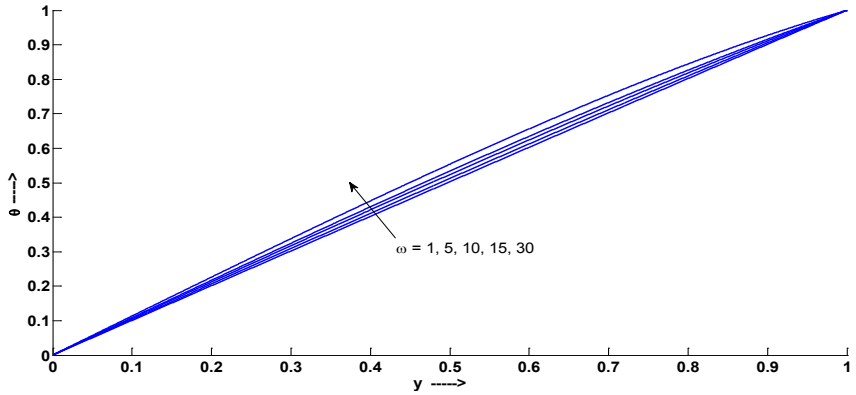

Figure 8 Temperature profiles for variation in ω when N = 2, E = 0.01, k = 0.5, ε = 0.2, Pr = 0.71.

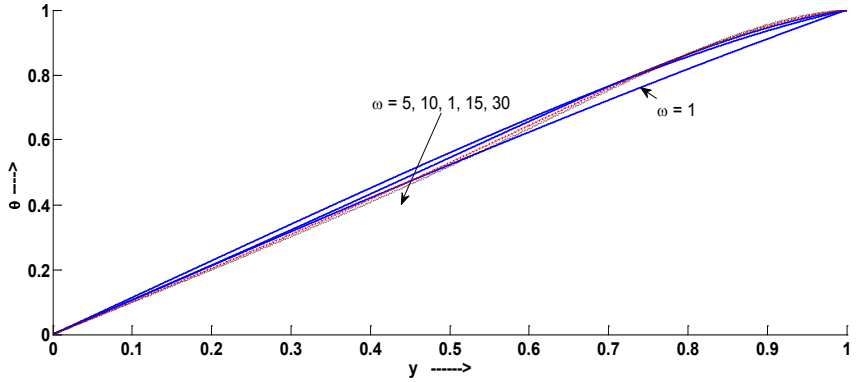

Figure 9 Temperature profiles for variation in ω when N = 2, E = 0.01, k = 0.5, ε = 0.2, Pr = 7.

Figures 10 and **11** depict the variation of transient temperature with respect to variation in radiation parameter N. It is clear that as N increases θ decreases in the case of air, and θ increases in the case of water. The radiation parameter N, being reciprocal of the Stark number (also known as the Stephan number), is the measure of relative importance of thermal radiation transfer to the conduction heat transfer. Thus, larger values of N indicate larger amounts of radiative energy being poured into the system. Hence, for fluids with low Prandtl number values, such as air, in which conductive heat transfer is stronger, an increase in N results in a decrease in velocity and temperature. In the case of water, where convective heat transfer is stronger, an increase in N results in velocity and temperature augmentation. **Figure 11** also shows that in the case of water, near a plate whose temperature is oscillating, the temperature θ in the channel decreases with a decrease in N.

The Prandtl number physically signifies the relative importance of momentum diffusion to thermal diffusion in the flow field. **Figure 12** shows the variation of temperature θ with respect to the Prandtl number Pr. It clearly shows that as the Prandtl number increases, temperature first increases and then decreases as we move towards the plate with oscillating plate temperature.

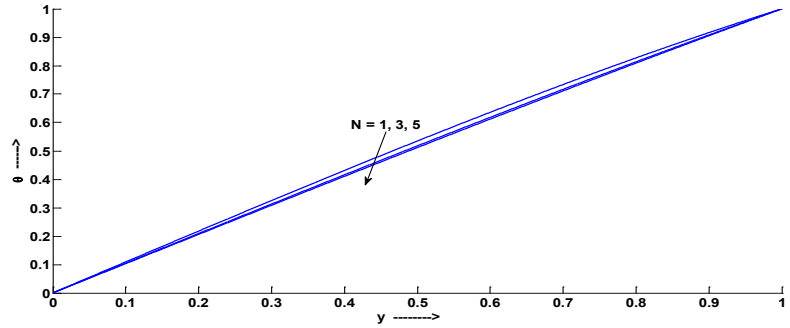

Figure 10 Temperature profiles for variation in N when ω = 10, E = 0.01, k = 0.5, ε = 0.2, Pr = 0.71.

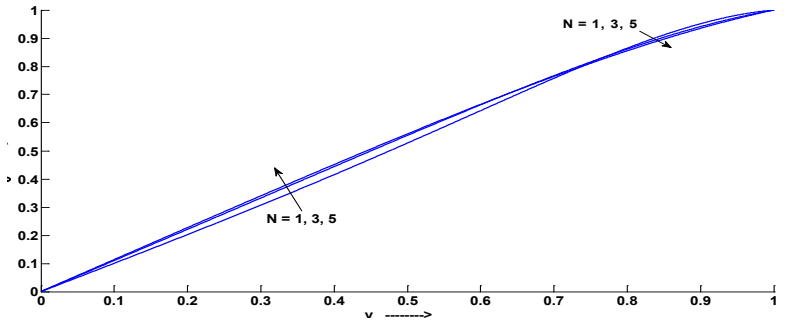

Figure 11 Temperature profiles for variation in N when ω = 10, E = 0.01, k = 0.5, ε = 0.2, Pr = 7.

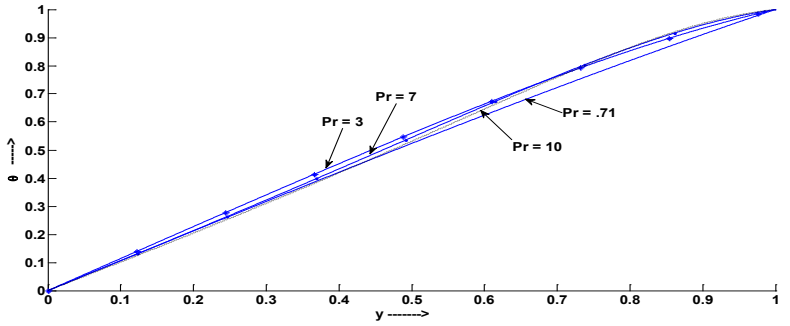

Figure 12 Temperature profiles for variation in Pr when N = 2, ω = 10, E = 0.01, k = 0.5, ε = 0.2.

The Eckeret number physically signifies the relative importance of viscous heating to thermal diffusion. Hence, larger values of Eckeret number indicate a greater impact of dissipation in the system. Here, we emphasize that dissipative effects are generally found to be weak when compared to other counterpart effects. Though dissipative effects may be quantitatively negligible in free convection, but they certainly show qualitative effects. In the present analysis, the effect of Eckert number on velocity and temperature has been shown through skin friction and wall temperature gradient simply because on

the present scale the effect is not quantitatively pronounced on velocity and temperature distributions. Hence, the effect of Eckeret number has been shown in tabular form in **Tables 1 - 4**.

The variation of amplitude B and tangent of phase angle tan(α) of skin friction coefficient with respect to various parameters is shown in **Figures 13 - 18** and their variation with respect to Eckeret number is shown in **Tables 1** and **2**.

Figure 13 shows that the amplitude of skin friction B decays considerably with the increasing values of ω for some range of values of ω, and beyond this range the variations are very moderate. The figure also reveals that B registers considerable decay with an increase in Pr values. **Figure 14** exhibits the effect of radiation N on B and reveals that for both air and water, B increases with an increase in N. The effect of permeability parameter k on B is depicted in **Figure 15,** which shows that B decays for both air and water for decreasing values of k.

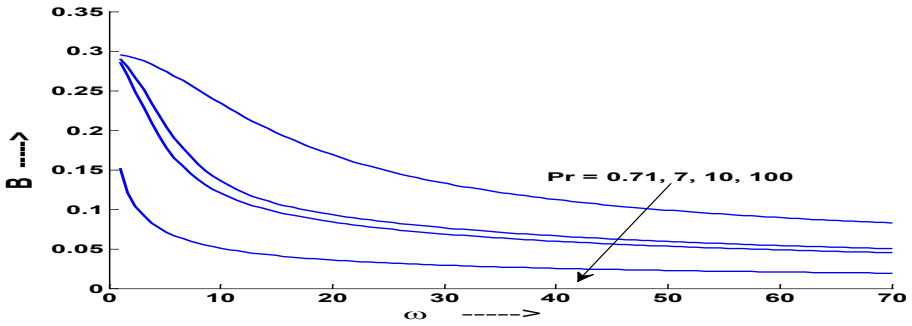

Figure 13 Variation in B with respect to ω for varying values of the Prandtl number when N = 2, E = 0.01, k = 0.5 and ϵ = 0.2.

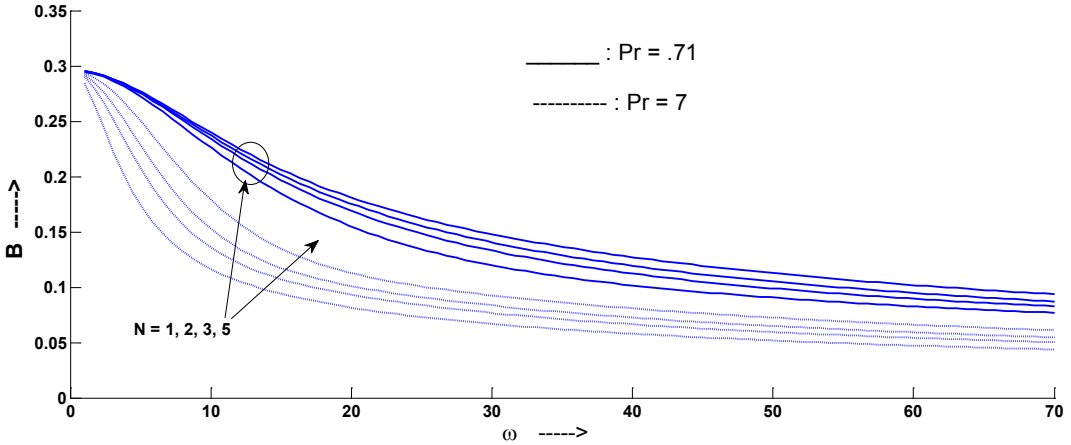

Figure 14 Variation in B with respect to ω for varying values of radiation parameter N both for air (Pr = 0.71) and water (Pr = 7) when E = 0.01, k = 0.5 and ϵ = 0.2.

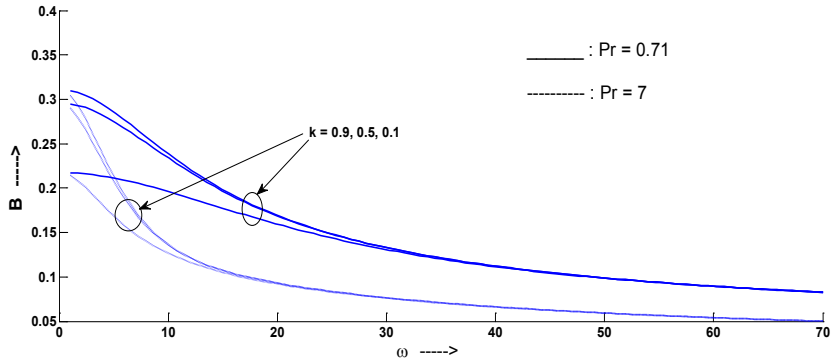

Figure 15 Variation in B with respect to ω for varying values of permeability parameter k both for air (Pr = 0.71) and water (Pr = 7) when E = 0.01, N = 2 and ϵ = 0.2.

Figure 16 displays the effect of the Prandtl number Pr and frequency ω on tan(α). It is observed that tan(α) decays uniformly with an increase in the Prandtl number for low frequency values, but some disturbances in the said trend is witnessed for the higher range of values of ω. **Figure 17** shows the variation in tan(α) with respect to radiation parameter N for air and water respectively, and indicates an increase in tan(α) with an increase in radiation parameter N for air. In the case of water, for small values of frequency, and after a certain critical value of frequency, this uniform variation gets disturbed. **Figure 18** executes variation in tan(α) with respect to the permeability parameter for both air and water. For air, with increasing values of the permeability parameter, tan(α) decreases in a regular fashion for rather larger values of frequencies, before becoming non responsive to frequency variation after a critical value of frequency. Contrarily, variation in tan(α) for water does not show much uniformity with respect to permeability.

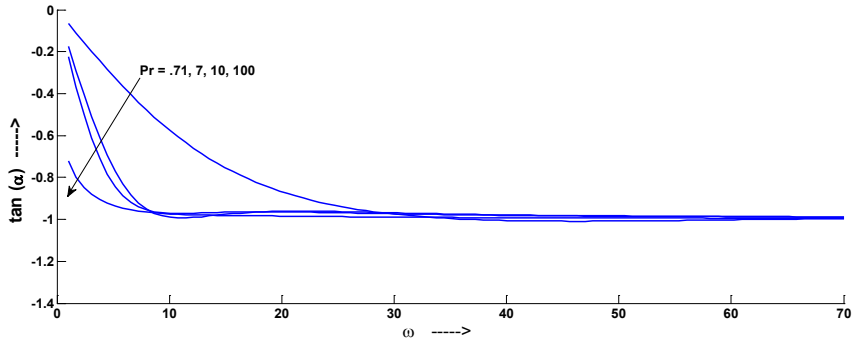

Figure 16 Variation in tan(α) with respect to ω for varying values of the Prandtl number when N = 2, E = 0.01, k= 0.5 and ϵ = 0.2.

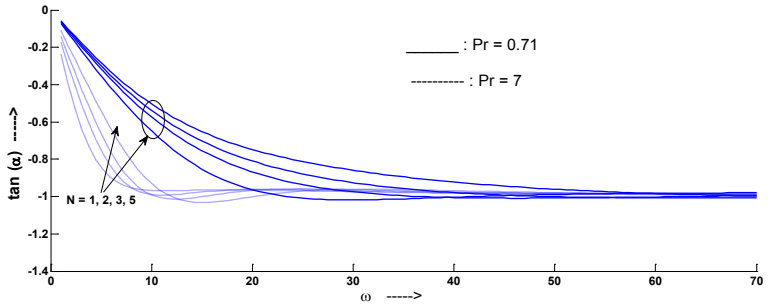

Figure 17 Variation in tan(α) with respect to ω for varying values of radiation parameter N both for air (Pr = 0.71) and water (Pr = 7) when E = 0.01, k = 0.5 and ϵ = 0.2.

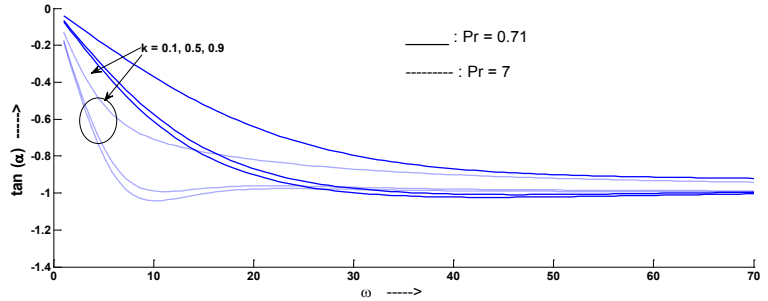

Figure 18 Variation in tan(α) with respect to ω for varying values of permeability parameter k both for air (Pr = 0.71) and water (Pr = 7) when E = 0.01,N = 2 and ϵ = 0.2.

Tables 1 and **2** show the variation in B and tan(α) with respect to the Eckeret number E for air and water, respectively. It may be inferred that though, for both air and water, B increases and tan(α) decreases with an increase in E, at high frequency both B and tan(α) decreases with an increase in E.

Table 1 Variation in B and tan(α) with respect to Eckeret number E when N = 2, Pr = 0.71, k = 0.5, ε = 0.2.

E	ω					
	B			tan(α)		
	5	19	40	5	19	40
.001	0.2751383892	0.1736475610	0.1122091094	-0.3157781537	-0.8492919559	-1.0054962974
.01	0.2751395063	0.1736474527	0.1122090313	-0.3157814620	-0.8492958154	-1.0054969520
.1	0.2751506765	0.1736463694	0.1122083164	-0.3158145443	-0.8493344111	-1.0055034984

Table 2 Variation in B and tan(α) with respect to Eckeret number E when N = 2, Pr = 7, k = 0.5, ε = 0.2.

E	ω					
	B			tan(α)		
	5	19	40	5	19	40
.001	0.2076562343	0.0954096388	0.0664063308	-0.7505799376	-0.9624925094	-0.9786136024
.01	0.2076563729	0.0954093699	0.0664062890	-0.7506326702	-0.9624931358	-0.9786138259
.1	0.2076577716	0.0954066815	0.0664058709	-0.7511601398	-0.9624993997	-0.9786160606

Figures 19 - 22 show the variation in amplitude and tangent of phase angle tan(β) of the Nusselt number for the plate undergoing temperature oscillations with respect to various parameters. **Tables 3** and **4** show their variation with respect to the Eckeret number.

Figure 19 displays the variation in the amplitude D of the Nusselt number for variable values of the Prandtl number Pr and frequency ω and exhibits that D increases with an increase in ω and Pr values. The increase is more pronounced for high Prandtl number values. **Figure 20** displays the effect of radiation parameter N on D and indicates that for both air and water D decreases with an increase in N.

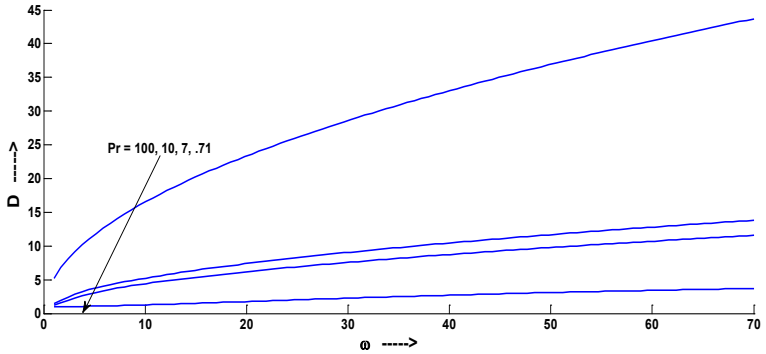

Figure 19 Variation in D with respect to ω for varying values of Prandtl number when N = 2, E = 0.01, k = 0.5 and ϵ = 0.2.

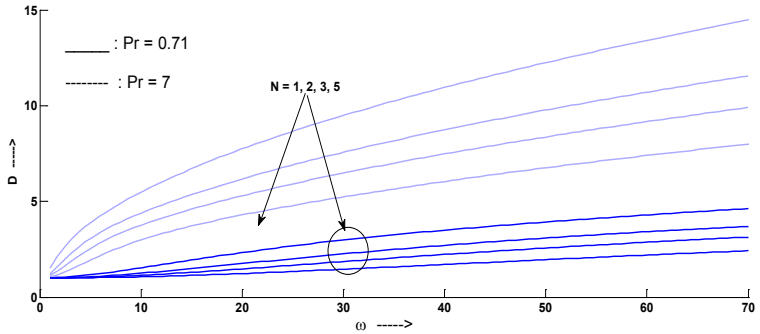

Figure 20 Variation in D with respect to ω for varying values of radiation parameter N both for air (Pr = 0.71) and water (Pr = 7) when E = 0.01, k = 0.5 and ϵ = 0.2.

The effect of frequency on tan(β) for different fluids warrants attention as can be seen in **Figure 21**; for air there is a smooth variation in tan(β) for large ranges of frequency values whereas for fluids having Prandtl number 7 and 10 there are sharp changes in tan(β) in a small range of frequency values. As Prandl number increases to 100 no variation in tan(β) occurs. **Figure 22** shows that tan(β) decreases with an increase in radiation parameter but fluctuations occur in the case of water.

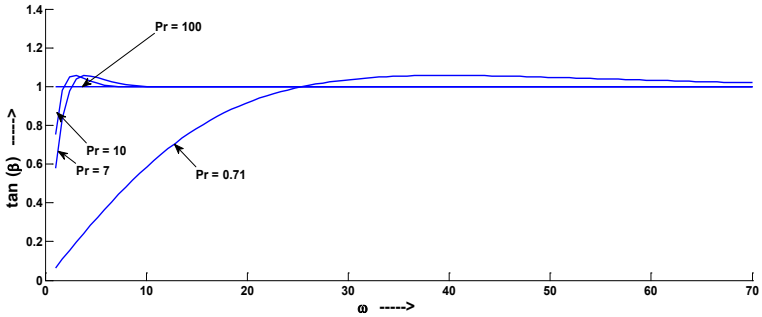

Figure 21 Variation in tan(β) with respect to ω for varying values of Prandtl number when N = 2, E = 0.01, k = 0.5 and ϵ = 0.2.

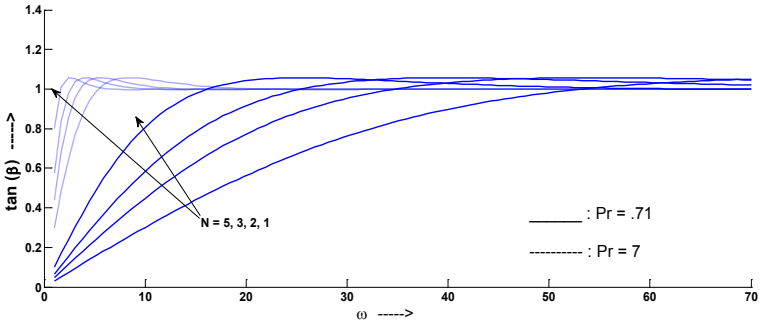

Figure 22 Variation in tan(α) with respect to ω for varying values of radiation parameter N both for air (Pr = 0.71) and water (Pr = 7) when E = 0.01, k = 0.5 and ϵ = 0.2.

Tables 3 and **4** show the variation in D and tan(β) with respect to the Eckeret number E for air and water, respectively. It may be inferred that though for both air and water D and tan(β) increases with an increase in E, at low frequency both D decreases and tan(β) increases with an increase in E only in the case of air.

Table 3 Variation in D and tan(β) with respect to Eckeret number E when N = 2, Pr = 0.71, k = 0.5, ε = 0.2.

E	ω					
	D			tan(β)		
	5	19	40	5	19	40
.001	1.0698789836	1.6999144620	2.7079296130	0.3143376634	0.8949218752	1.0573438328
.01	1.0698521287	1.6999224539	2.7079362511	0.3143645980	0.8949411558	1.0573481084
.1	1.0695836151	1.7000023835	2.7080026328	0.3146340415	0.8951339719	1.0573908641

Table 4 Variation in D and tan(β) with respect to Eckeret number E when N = 2, Pr = 7, k = 0.5, ε = 0.2.

E	ω					
	D			tan(β)		
	5	19	40	5	19	40
.001	3.0633833656	6.0212047432	8.7387040732	1.0488757988	0.9993712011	1.0000039566
.01	3.0634790149	6.0212352334	8.7387190948	1.0490041822	0.9993822570	1.0000076313
.1	3.0644361386	6.0215401458	8.7388693126	1.0502884812	0.9994928168	1.0000443780

Conclusions

Unsteady oscillatory free convection flow of radiative dissipative viscous incompressible fluid in a long vertical parallel plate channel filled with porous medium has been analyzed. Both the plates of the channel were stationary and the temperature of one of the plates oscillated about a constant non zero mean temperature. The study results give the following conclusions:

1. At high frequency values, an increase in frequency leads to a decrease in transient velocity for both air and water.
2. Velocity of air decreases while that of water increases with an increase in radiation parameter.
3. The fluid velocity increases with an increase in permeability parameter and a decrease in the Prandtl number respectively.
4. The effects of fluctuations in temperature are more prominent in the region proximate to the channel wall having oscillatory plate temperature.
5. An increase in frequency leads to an increase in transient temperature in the case of air while leading to a decrease in transient temperature in the case of water.
6. The fluid temperature for air decreases and that of water increases with an increase in radiation parameter.
7. With an increase in the Prandtl number, the temperature of the fluid decreases.
8. The magnitude and the tangent of the phase angle of the skin friction coefficient increases with a decrease in frequency and Prandtl number. They also increase with an increase in radiation parameter. However, these quantities witness a decrease with an increase in the Eckeret number for high frequency values. The magnitude of skin friction coefficient decays and the tangent of the phase angle of the skin friction coefficient increases with a decrease in the Eckeret number for low frequency values and a decrease in the permeability parameter.
9. The magnitude and the tangent of the phase angle of the Nusselt number increases with an increase in frequency and Prandtl number. These quantities of interest also decrease with an increase in radiation parameter. The magnitude and the tangent of the phase angle of the Nusselt number increase with an increase in the Eckeret number for water and at only high frequency values in the case of air. The magnitude of the skin friction coefficient decreases and the tangent of the phase angle of the skin friction coefficient increases with an increase in the Eckeret number for low frequency values in the case of air.

References

[1] PS Ghoshdastidar. *Heat Transfer.* Oxford University Press, Oxford, 2004.
[2] DA Nield and A Bejan. *Convection in Porous Media*. Springer, New York, 2006.
[3] FP Incropera, DP Dewitt, TL Bergman and SL Adrieme. *Fundamentals of Heat and Mass Transfer*. 6th (ed.). John Wiley & Sons, India, 2011.
[4] S Ostrach. Laminar natural convection flow and heat transfer of fluids with and without heat sources in channels with constant wall temperatures. National Advisory Committee for Aeronautics, United States, 1952, p. 1-55.
[5] W Aung. Fully developed laminar free convection between vertical plates heated asymmetrically. *Int. J. Heat Mass Tran.* 1972; **15**, 1577-80.
[6] O Miyatake and T Fuji. Free convection heat transfer between vertical plates-one plate isothermally heated and other thermally insulated. *Heat Tran. Jap. Res.* 1972; **1**, 30-8.
[7] H Nakamura, Y Asako and T Naitou. Heat Transfer by free convection between two parallel flat plates. *Numer. Heat Tran.* 1982; **5**, 95-106.
[8] W Aung and G Worku. Developing flow and flow reversal in a vertical channel with asymmetric wall temperatures. *J. Heat Tran.* 1986; **108**, 299-304.
[9] DJ Nelson and BD Wood. Fully developed combined heat and mass transfer natural convection between vertical parallel plates with asymmetric boundary conditions. *Int. J. Heat Mass Tran.* 1989; **32**, 1789-92.
[10] J Hernandez and B Zamora. Effects of variable properties and non-uniform heating on natural convection flows in vertical channels. *Int. J. Heat Mass Tran.* 2005; **48**, 793-807.
[11] A Pantokratoras. Fully developed laminar free convection with variable thermo-physical properties between two open-ended vertical parallel plates heated asymmetrically with large temperature differences. *Trans. ASME* 2006; **128**, 405-8.
[12] DF Delmastro, AF Chasseur and JC Garcia. Fully developed laminar convection with variable thermophysical properties between two heated vertical parallel plates. *Lat. Am. Appl. Res.* 2009; **39**, 85-90.
[13] N Rudriah and ST Nagraj. Natural convection through vertical porous stratum. *Int. J. Eng. Sci.* 1977; **15**, 589-600.
[14] A Raptis and N Kafousias. Heat transfer in flow through a porous medium bounded by an infinite vertical plate under the action of a magnetic field. *Energy Res.* 1982; **6**, 241-5.
[15] MA Hossain and I Pop. Radiation effects on free convection over a vertical flat plate embedded in a porous medium with high porosity. *Int. J. Therm. Sci.* 2001; **40**, 289-95.
[16] A Raptis. Radiation and free convection flow through a porous medium. *Int. Comm. Heat Mass Tran.* 2009; **25**, 289-95.
[17] RS Nanda and VP Sharma. Free convection laminar boundary layers in oscillatory flow. *J. Fluid Mech.* 1963; **15**, 419-28.
[18] A Raptis and CP Perdikis. Oscillatory flow through a porous medium by the presence of free convective flow. *Int. J. Eng. Sci.* 1985; **23**, 51-5.
[19] OD Makinde and PY Mhone. Heat Transfer to MHD oscillatory flow in a channel filled with porous medium. *Rom. J. Phys.* 2005; **50**, 931-8.
[20] JC Umavati, A Mateen, AJ Chamka and AA Mudhaf. Oscillatory Hartmann two fluid flow and heat transfer in a horizontal channel. *Int. J. Appl. Mech. Eng.* 2006; **11**, 155-78.
[21] P Vyas and A Ranjan. Dissipative MHD boundary layer flow in a porous medium over a sheet stretching non linearly in the presence of radiation. *Appl. Math. Sci.* 2010; **4**, 3133-42.
[22] P Vyas and N Srivastava. On dissipative radiative MHD boundary layer flow in a porous medium over a non-isothermal stretching sheet. *J. Appl. Fluid Mech.* 2012; **5**, 23-31.
[23] R Grief, IS Habib and JC Lin. Laminar convection of a radiating gas in a vertical channel. *J. Fluid Mech.* 1971; **46**, 513-20.
[24] AR Vijaylakshmi. Radiation effects on free convection flow past an impulsively started vertical plate in a rotating fluid. *Theor. Appl. Mech.* 2010; **37**, 79-95.

[25] CFKettleborough. Transient laminar free convection between heated vertical plates including entrance effects. *Int. J. Heat Mass Tran.* 1972; **15**, 883-96.
[26] HM Joshi. Transient effects in natural convection cooling of vertical parallel plates. *Int. Comm. Heat Mass Tran.* 1988; **15**, 227-38.
[27] T Paul, BK Jha and AK Singh. Transient free convection flow in a vertical channel with constant heat flux on walls. *Heat Mass Tran.* 1996; **32**, 61-3.
[28] AK Singh, HR Gholami and V M Soundalgekar. Transient free convection flow between two vertical parallel plates. *Heat Mass Tran.* 1996; **31**, 329-32.
[29] AK Singh and T Paul. Transient natural convection between two vertical walls heated/cooled asymmetrically. *Int. J. Appl. Mech. Eng.* 2006; **11**, 143-54.
[30] A Andreozzi, B Buonomo and O Manca. Transient natural convection in vertical channels symmetrically heated at uniform heat flux. *Numer. Heat Tran.: Part A* 2009; **55**, 409-31.
[31] A Al-Subaie Mansour and AJ Chamka. Transient natural convection flow of a particulate suspension through a vertical channel. *Heat Mass Tran.* 2004; **40**, 707-13.
[32] DA Nield. Resolution of a paradox involving viscous dissipation and non-linear drag in a porous medium. *Transport Porous Media* 2000; **41**, 349-57.
[33] AK Al-Hadhrami, DB Elliot and DB Ingham. A new model for viscous dissipation in porous media across a range of permeability values. *Transport Porous Media* 2003; **53**, 117-22.
[34] M Narahari. Oscillatory plate temperature effects of free convection flow of dissipative fluid between long vertical parallel plates. *Int. J. Appl. Math. Mech.* 2009; **5**, 30-46.

Appendix

$$N_1 = \frac{1}{1+\frac{4N}{3}}, \quad k_1 = \frac{1}{\sqrt{k}}, \quad R_1 = \sqrt{i\omega \Pr N_1}, \quad R_2 = \sqrt{i\omega + k_1^2}, \quad R_3 = R_2^2 - R_1^2$$

$$R_4 = (k_1 + R_2)^2 - R_1^2, \quad R_5 = (k_1 - R_2)^2 - R_1^2, \quad R_6 = k_1^2 + 2k_1R_1, \quad R_7 = k_1^2 - 2k_1R_1$$

$$R_8 = k_1^2 + 2R_2k_1, \quad R_9 = k_1^2 - 2R_2k_1, \quad R_{10} = k_1 + R_1, \quad R_{11} = k_1 + R_2, \quad R_{12} = k_1 - R_1$$

$$R_{13} = k_1 - R_2, \quad R_{14} = (k_1 + R_1)^2 - R_2^2, \quad R_{15} = (k_1 - R_1)^2 - R_2^2$$

$$T_2 = \Pr N_1\left[\frac{k^2}{4\sinh^2(k_1)} + \frac{2k^2}{k_1\sinh(k_1)}\right]$$

$$T_1 = -T_2 + \Pr N_1\left[\frac{k^2\cosh(2k_1)}{4\sinh^2(k_1)} + \frac{2k^2\cosh(k_1)}{k_1\sinh(k_1)} - \frac{3k^2}{2} + \frac{k}{12}\right]$$

$$T_3 = -T_2k - \Pr N_1\left[\frac{k^3}{12\sinh^2(k_1)} - 3k^4\right]$$

$$T_4 = -T_3\coth(k_1) - T_1k\cos ech(k_1) - \frac{\Pr N_1}{\sinh(k_1)}\left[\frac{k^3\cosh(2k_1)}{12\sinh^2(k_1)} - \frac{k^2\coth(k_1)}{2k_1} - \frac{k^2}{12} - 3k^4\right]$$

$$T_5 = \frac{2\Pr N_1}{R_3}\left[\frac{-kR_2}{R_3\sinh(R_2)} - \frac{kk_1R_1(1/R_6 + 1/R_7)}{2\sinh(k_1)\sinh(R_1)} + \frac{kk_1R_2(1/R_4 + 1/R_5)}{2\sinh(k_1)\sinh(R_2)} + \frac{2R_2}{R_3^2\sinh(R_2)} - \frac{(1/R_6 - 1/R_7)}{2\sinh(k_1)\sinh(R_1)} + \frac{(1/R_4 - 1/R_5)}{2\sinh(k_1)\sinh(R_2)}\right]$$

$$T_6 = -T_5\coth(R_1) + \frac{2\Pr N_1}{R_3\sinh(R_1)}\left[k/2 - (kR_2/R_3)\coth(R_2) + \frac{\coth(R_1)}{4R_1} - \frac{1}{4R_1^2} - \frac{1}{R_3} - \frac{kk_1R_1(\cosh(R_{10})/R_6 + \cosh(R_{12})/R_7)}{2\sinh(k_1)\sinh(R_1)} + \frac{2R_2\coth(R_2)}{R_3^2}\right.$$
$$\left. + \frac{kk_1R_2(\cosh(R_{11})/R_4 + \cosh(R_{13})/R_5)}{2\sinh(k_1)\sinh(R_2)} - \frac{(\cosh(R_{10})/R_6 - \cosh(R_{12})/R_7)}{2\sinh(k_1)\sinh(R_1)} + \frac{(\cosh(R_{11})/R_4 - \cosh(R_{13})/R_5)}{2\sinh(k_1)\sinh(R_2)}\right]$$

$$T_7 = \frac{-T_5}{R_3} - \frac{2\Pr N_1}{R_3}\left[\frac{-kR_1}{R_3^2\sinh(R_1)} - \frac{kk_1R_1(1/(R_6R_{14}) + 1/(R_7R_{15}))}{2\sinh(k_1)\sinh(R_1)} + \frac{kk_1R_2(1/(R_8R_4) + 1/(R_9R_5))}{2\sinh(k_1)\sinh(R_2)} - \frac{(8R_1^2/R_3^2 + 2/R_3)}{4R_1R_3\sinh(R_1)}\right.$$
$$\left. + \frac{1}{2R_1R_3^2\sinh(R_1)} - \frac{(1/(R_6R_{14}) - 1/(R_7R_{15}))}{2\sinh(k_1)\sinh(R_1)} + \frac{(1/(R_8R_4) + 1/(R_9R_5))}{2\sinh(k_1)\sinh(R_2)}\right]$$

$$T_8 = -T_7 \coth(R_2) - \frac{T_5 \cosh(R_1)}{R_3 \sinh(R_2)} - \frac{T_6 \sinh(R_1)}{R_3 \sinh(R_2)} - \frac{2 \Pr N_1}{R_3}[\frac{-k}{2R_3} - \frac{k}{2R_3} - \frac{kR_1 \coth(R_1)}{R_3^2} - \frac{kk_1R_1}{2\sinh(k_1)\sinh(R_1)}(\frac{\cosh(R_{10})}{R_{14}R_6} + \frac{\cosh(R_{12})}{R_{15}R_7})$$
$$+ \frac{kk_1R_2}{2\sinh(k_1)\sinh(R_2)}(\frac{\cosh(R_{11})}{R_8R_4} + \frac{\cosh(R_{13})}{R_9R_5}) - \frac{\coth(R_1)(1 + 8R_1^2/R_3^2 + 2/R_3)}{4R_1R_3} + \frac{(\sinh(R_1) + (2R_1/R_3)\cosh(R_1))}{4R_1^2R_3\sinh(R_1)}$$
$$- \frac{(\cosh(R_2) - \sinh(R_2)/R_2)}{4R_2R_3\sinh(R_2)} - \frac{1}{2\sinh(k_1)\sinh(R_1)}(\frac{\cosh(R_{10})}{R_{14}R_6} - \frac{\cosh(R_{12})}{R_{15}R_7}) + \frac{1}{2\sinh(k_1)\sinh(R_2)}(\frac{\cosh(R_{11})}{R_8R_4} - \frac{\cosh(R_{13})}{R_9R_5})]$$

$$A = k(1 - k_1\coth(k_1)) + E(T_3k_1\sinh(k_1) + T_4k_1\cosh(k_1) + (T_1 - T_2)k + \Pr N_1(\frac{k_1k^3\sinh(2k_1)}{6\sinh^2(k_1)} - k^2(\frac{1}{k_1} + \frac{3kk_1}{2})\coth(k_1) - \frac{5k^2}{6} - \frac{3k^3}{2}))$$

$$B = \frac{R_1\coth(R_1)}{R_3} - \frac{R_2\coth(R_2)}{R_3} + E(T_7R_2\sinh(R_2) + T_8R_2\cosh(R_2) + \frac{T_5R_1\sinh(R_1)}{R_3} + \frac{T_6R_1\cosh(R_1)}{R_3} +$$
$$\frac{2\Pr N_1}{R_3}(\frac{-k}{R_3} - \frac{-kR_1\coth(R_1)}{2R_3} - \frac{kR_1^2}{R_3^2} - \frac{kR_2\coth(R_2)}{2R_3} + \frac{1}{4R_1^2R_3} + \frac{1}{2R_3^2} - \frac{kk_1R_1}{2\sinh(k_1)\sinh(R_1)}(\frac{R_{10}\sinh(R_{10})}{R_{14}R_6} + \frac{R_{12}\sinh(R_{12})}{R_{15}R_7})$$
$$+ \frac{kk_1R_2}{2\sinh(k_1)\sinh(R_2)}(\frac{R_{11}\sinh(R_{11})}{R_8R_4} + \frac{R_{13}\sinh(R_{13})}{R_9R_5}) - \frac{\coth(R_1)}{4R_3}(1 + \frac{8R_1^2}{R_3^2} + \frac{2}{R_3}) - \coth(R_1)(\frac{1}{2R_1R_3} + \frac{R_1}{R_3^2} - \frac{1}{4R_1R_3})$$
$$- \coth(R_2)(\frac{1}{4R_2R_3} + \frac{R_2}{R_3^2}) + \frac{1}{4R_2^2R_3} - \frac{1}{4R_3} - \frac{1}{2\sinh(k_1)\sinh(R_1)}(\frac{R_{10}\sinh(R_{10})}{R_{14}R_6} - \frac{R_{12}\sinh(R_{12})}{R_{15}R_7})$$
$$+ \frac{1}{2\sinh(k_1)\sinh(R_2)}(\frac{R_{11}\sinh(R_{11})}{R_8R_4} - \frac{R_{13}\sinh(R_{13})}{R_9R_5})))$$

$$C = -1 + E\Pr N_1(\frac{k^2k_1\sinh(2k_1)}{2\sinh^2(k_1)} - 2k^2k_1\coth(k_1) + k^2 + \frac{k}{3}) - ET_1$$

$$D = \frac{2E\Pr N_1}{R_3}(\frac{k}{2} + \frac{kR_1\coth(R_1)}{2} - \frac{kR_2^2}{R_3}) + \frac{\coth(R_1)}{2R_1} + \frac{1}{4} - \frac{1}{4R_1^2} - \frac{1}{R_3} - \frac{kk_1R_1}{2\sinh(k_1)\sinh(R_1)}(\frac{R_{10}\sinh(R_{10})}{R_6} + \frac{R_{12}\sinh(R_{12})}{R_7}) - \frac{y\coth(R_1)}{4R_1}$$
$$+ \frac{kk_1R_2}{2\sinh(k_1)\sinh(R_2)}(\frac{R_{11}\sinh(R_{11})}{R_4} + \frac{R_{13}\sinh(R_{13})}{R_5}) - \frac{yR_2\coth(R_2)}{R_3} - \frac{1}{2\sinh(k_1)\sinh(R_1)}(\frac{R_{10}\sinh(R_{10})}{R_6} - \frac{R_{12}\sinh(R_{12})}{R_7}) + \frac{2R_2^2}{R_3^2}$$
$$+ \frac{1}{2\sinh(k_1)\sinh(R_2)}(\frac{R_{11}\sinh(R_{11})}{R_4} - \frac{R_{13}\sinh(R_{13})}{R_5}))$$